OBJECT SHAPE RECOGNITION WITH ARTIFICIAL WHISKERS USING TOMOGRAPHIC RECONSTRUCTION

Cagdas Tuna,[1] *Joseph H. Solomon,*[2] *Douglas L. Jones,*[1] *and Mitra J. Z. Hartmann*[2,3]

[1]Department of Electrical and Computer Engineering,
University of Illinois at Urbana-Champaign, Urbana, IL 61801, USA
Departments of [2]Mechanical Engineering and [3]Biomedical Engineering,
Northwestern University, Evanston, IL 60208, USA

ABSTRACT

Existing techniques utilizing bio-inspired robotic whisker sensory systems generally address object feature extraction with artificial whiskers as a mechanical problem. We present an alternative signal-processing approach that formulates the object shape recognition as a 2-D tactile imaging problem. Observing that the whisker position at the very initial contact is similar to a 'ray path' in X-ray computed tomography; the 2-D cross-sectional image of the object can be tomographically reconstructed by measuring only the angle at the whisker base and the whisker-base location at the initial contact for each viewing angle. This approach has the important practical advantage of eliminating the need for the calibration of the force/moment measurements. Experimental results demonstrate the promising potential for bio-inspired systems using arrays of vibrissal sensors for object shape recognition.

Index Terms— Artificial whiskers, tomography, image reconstruction, bio-inspired signal processing, shape recognition

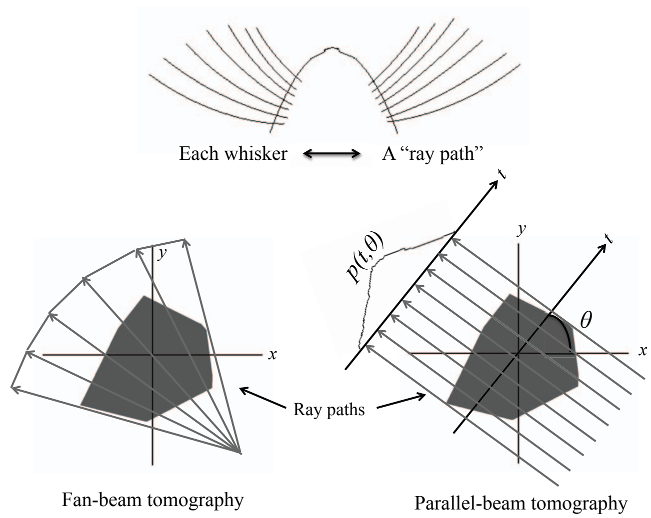

Fig. 1. Whisker tomography: The paths on which whiskers lie are similar to projection 'ray paths' in X-ray computed tomography.

1. INTRODUCTION

Vibrissal-sensing animals (including rats, shrews, and seals) use their whiskers for navigation and exploration of their surroundings [1, 2]. Rats are able to extract object features and fluid-flow velocity very precisely through oscillatory motions of their whiskers [3, 4]. Inspired by the animal world, there are several recent studies that use artificial whiskers for object feature extraction. Clements and Rahn [5] developed a flexible whisker with a two-axis actuator and six-axis force/torque sensor based on an elastic model to determine contact point locations. Solomon and Hartmann [6] designed a whisker array, combining the data for tactile extraction of three-dimensional object shape by taking lateral slip and surface friction into account. They also derived a sweeping algorithm to map the detailed profile of objects with a robotic whisker using the torque information [7].

We present a new 2-D tomographic reconstruction approach to the problem of object shape recovery with robotic whiskers. In X-ray computed tomography (CT), X-rays pass through the interior of the object along straight lines, or 'ray paths', from different directions. The projections at a particular angular view are the set of line integrals taken over these ray paths [8, 9]. Analogously, in our method called 'whisker tomography', we apply the tomography idea by considering the the whisker position at the very initial contact as a projection 'whisker path' as illustrated in Figure 1.

Whisker tomography differs from the standard tomography in terms of projection data collection because the whisker always makes contact with the object at a discrete point along its length, eliminating the need for line integrals. On the other hand, contrary to the X-ray CT, the projection vector is very sparse at any viewing angle, since there are no such 'whisker paths' passing through the interior of the object. To address this type of limited-data tomography problem, we apply a basic clustering approach, considering the whisker path at the initial contact as a boundary layer, which separates the region where the whisker moves freely from the region where the whisker bends following the initial contact with the object.

2. WHISKER TOMOGRAPHY

Our method assumes the 2-D imaging of fixed, rigid convex objects using an artificial whisker that is made of a thin, flexible, straight, cylindrical beam. The whisker bends only within its plane of rotation and makes contact with the object at a single point along its length, not at its tip. Two strain gages are attached to the whisker at its base, facing against each other to measure the electrical resistance change caused by bending. Different from the techniques based on the cantilever beam theory, our method eliminates the calibration procedure for the moment/force measurements because we only need the information about the angle at the whisker base, not the actual value of the moments/forces.

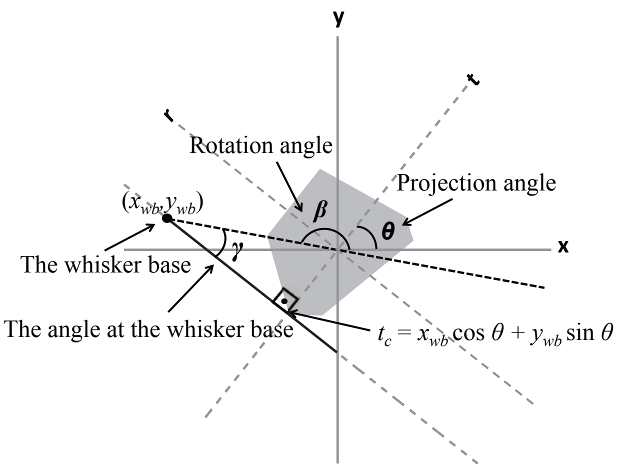

Fig. 2. The whisker position at the initial contact with an unknown object at the viewing angle θ: The angle at the whisker base, γ, and the whisker rotation angle, β, are recorded to compute the projection angle, θ, using Equation (1).

The voltage level measured at the whisker base starts increasing when the whisker makes the initial object contact. Therefore, the first step is to record the angle at the whisker base at the beginning of the voltage rise. The relation between the angle at the whisker base γ and the projection angle θ is illustrated in Figure 2 and can be defined mathematically as

$$\theta = \mod(-\gamma + \beta + 90^\circ, 180^\circ) \tag{1}$$

where β represents the amount of whisker rotation since the initial position of the whisker at the first angular view, taking values between 0° and 360°. The mod denotes the modulo operation and is applied to shrink the projection angles into

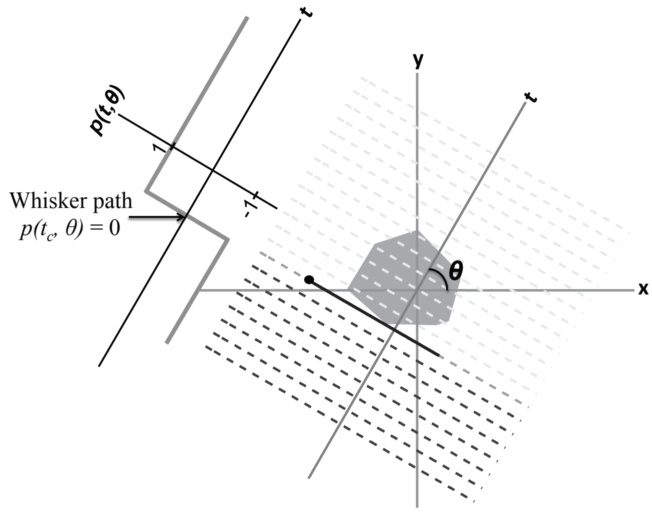

Fig. 3. Projection assignment at a particular viewing angle θ using a basic clustering approach: The whisker path is regarded as a boundary layer that separates the region that contains the object from the free-whisking region, so that we assign zero to the element in the projection vector corresponding to the whisker path. It is reasonable to choose a negative value for the projection vector elements associated with the free-whisking region and a positive value for the region surrounding the object. The elements in the projection vector take values from the set $\{-1, 0, 1\}$.

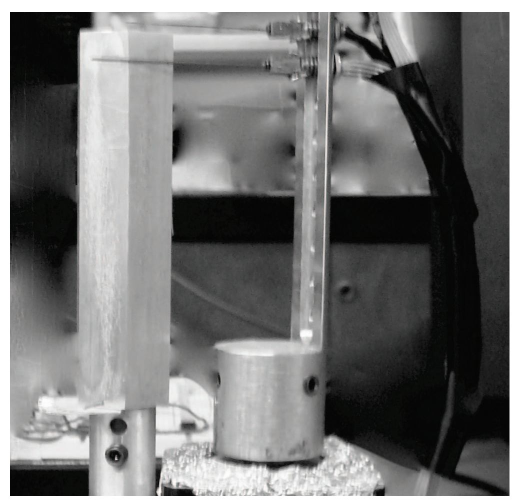

Fig. 4. The experimental setup. The whisker was rotated against the objects that were made of aluminum bars with three different cross sections including circle, hexagon and square.

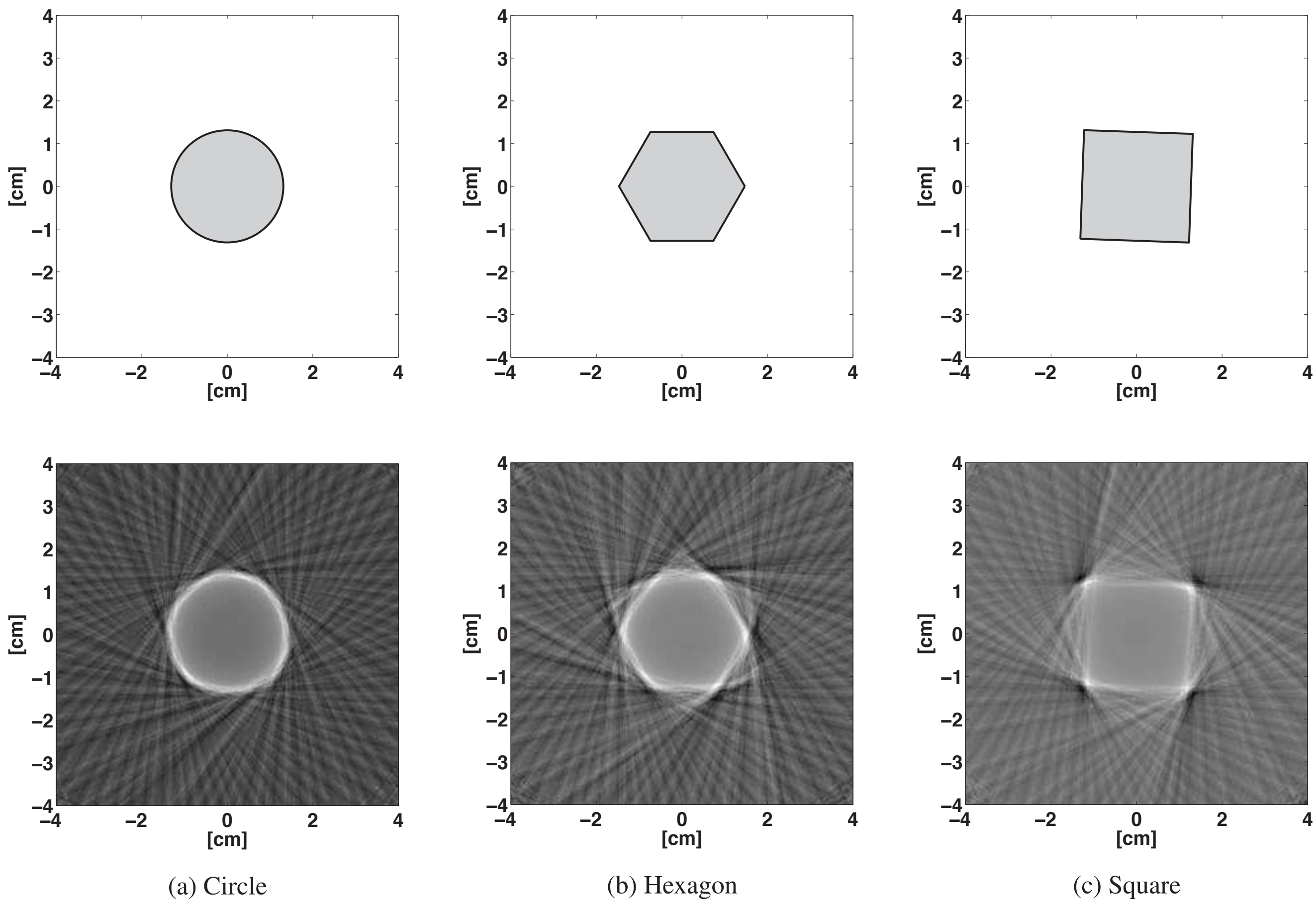

Fig. 5. Results of object shape recognition with whisker tomography. Top row: 2-D positions of the actual objects including circle, hexagon and square. Bottom row: the resulting object images obtained by applying whisker tomography. A total of 72 whisks were performed at evenly spaced (5°) intervals around the objects.

the range between 0° and 180° for tomographic reconstruction. As also shown in Figure 2, the position t_c of the 'whisker path' in the rotated (t, r) coordinate system can be computed by using the location of the whisker base (x_{wb}, y_{wb}) at the initial contact:

$$t_c = \quad x_{wb} \cos\theta + y_{wb} \sin\theta \tag{2}$$

Figure 3 illustrates the basic clustering approach based on assigning discrete values to the missing projection data. The whisker moves freely until the initial contact with the object occurs, whereas the whisker begins to bend as it moves along the object past the initial contact, revealing that the object is somewhere inside the region beyond the the initial contact. As a result, the 'whisker path' on which the whisker lies serves as a transition/boundary layer, providing information about the object contours. Therefore, at a particular angular view, it is reasonable to assign zero to the element in the projection vector associated with the whisker path and subsequently set a negative for the projection-vector elements corresponding to the region where the whisker moves freely, since during the tomographic image reconstruction, it makes sense to attenuate the pixels which are not related with the object. Similarly, in order to intensify the pixels representing the object in the final reconstructed image, a positive value is given to the projection vector elements denoting the region where the whisker cannot move any further without bending. Accordingly, we find that it is convenient to pick $\{-1, 0, 1\}$ as the projection values for these three situations.

Following the projection assignment step, we apply standard reconstruction algorithms for the parallel-beam tomography such as the filtered back-projection (FBP) to reconstruct the final 2-D cross-sectional image of the object. The FBP reconstruction formula for an image $s(x, y)$ is [8, 9]

$$s(x, y) = \int_0^{\pi} \int_{-\infty}^{\infty} P(f, \theta)|f|e^{j2\pi ft} df d\theta \tag{3}$$

3. EXPERIMENTAL RESULTS

We used the same setup used in previous experiments to test our tomographic approach for object shape recognition [6, 7]. The robotic whisker is made up of a superelastic Nitinol ($E \approx 8 \times 10^4$ MPa) wire, which is 0.5 mm in diameter and 5 cm in length. The whisker was attached to a small aluminum block ($4 \times 4 \times 8$ mm) with a strain gage superglued to each of its four faces although only two of these strain gages are used as we restrict the whisker bending into its axis of rotation, considering only 2-D cross-sectional imaging of the objects. The aluminum block was attached to an aluminum bar with a set screw, and the whole setup was mounted on an AC servomotor with a quadrature encoder with 2048 counts/revolution for actuation.

We did not perform any calibration trials as we did not need to measure the moment at the whisker base. All the measured data was low-pass filtered at 160 Hz, sampled at 1 kHz, and passed through a zero-phase digital filter with a cut-off frequency of 50 Hz.

We tested our method for the 2-D imaging of the objects that were made of aluminum bars with three different cross sections including circle, hexagon and square. As shown in Figure 4, the whisker base was positioned about 4 cm to the right of test object centers. The pulses were sent to the AC servomotor at 100 Hz and the whisker was rotated against the object until a small amount of bending is attained, immediately retracting back to its initial position at rest. For experimental purposes, rather than moving the whisker around the stationary object for the next angular view, we rotated the object about its center by $5°$ while keeping the whisker base fixed in space. This is simply the same as having the whisker base move around the object circularly.

A 256×256 image matrix was used for tomographic reconstruction. The whisker was rotated by $5°$ between two consecutive whisks, completely scanning the region surrounding the object through $360°/5° = 72$ whisks. Figure 5 shows the resulting images obtained by applying tomographic reconstruction. The results demonstrate that the tomographic imaging concept can be successfully applied to extract two-dimensional object features including shape, size and location using robotic whiskers as we were able to achieve accurate images of the object shapes.

4. CONCLUSION

In this paper, we introduce a new 2-D tomographic imaging approach to the existing problem of object shape extraction using artificial whiskers. To our knowledge, the literature applying signal processing methods on imaging of surroundings with vibrissal sensors is minimal. The results strongly indicate that our model has a future potential of practical use as we successfully adapt a well-studied imaging technique to a very different problem, which has been generally addressed from a mechanical point of view. Artifacts observed as line strips in the background are solely due to using the standard FBP algorithm for image reconstruction. Therefore, future studies include developing more complex image reconstruction techniques to reduce the image artifacts by exploiting the sparse nature of the whisking problem.

5. ACKNOWLEDGMENTS

This research is funded by NSF EFRI-BSBA Award #0938007.

6. REFERENCES

[1] F. Anjum, H. Turni, P. G. H. Mulder, J. V. D. Burg, and M. Brecht, "Tactile guidance of prey capture in etruscan shrews," in *Proc. Nat. Acad. Sci. USA*, vol. 103, Oct. 31 2006, pp. 16 544–16 549.

[2] G. Dehnhardt, B. Mauck, and H. Bleckmann, "Seal whiskers detect water movements," *Nature*, vol. 394, pp. 235–236, July 16 1998.

[3] M. L. Andermann, J. Ritt, M. A. Neimark, and C. I. Moore, "Neural correlates of vibrissa resonance: band-pass and somatotopic representation of high-frequency stimuli," *Neuron*, vol. 42, pp. 451–463, 2004.

[4] M. Brecht, B. Preilowski, and M. Merzenich, "Functional architecture of the mystacial vibrissae," *Behav Brain Res*, vol. 84, pp. 81–97, 1997.

[5] T. N. Clements and C. D. Rahn, "Three dimensional contact imaging with an actuated whisker," *IEEE Transactions on Robotics*, vol. 22, no. 4, pp. 844–848, 2006.

[6] J. H. Solomon and M. J. Z. Hartmann, "Artificial whiskers suitable for array implementation: Accounting for lateral slip and surface friction," *IEEE Transactions on Robotics*, vol. 24, no. 5, pp. 1157–1167, October 2008.

[7] ——, "Extracting object contours with the sweep of a robotic whisker using torque information," *The International Journal of Robotics Research*, vol. 29, no. 9, pp. 1233–1245, August 2010.

[8] R. E. Blahut, *Theory of Remote Image Formation*. Cambridge, UK: Cambridge University Press, 2004.

[9] J. Hsieh, *Computed Tomography: Principles, design, artifacts, and recent advances*. Bellingham, WA: SPIE-The International Society for Optical Engineering, 2003.